AD-A103 307 COLORADO UNIV AT BOULDER DEPT OF AEROSPACE ENGINEERI--ETC F/G 20/4
TRANSONIC SHOCK - TURBULENT BOUNDARY LAYER INTERACTION AND INCI--ETC(U)
JUN 81 G R INGER N00014-80-C-0470

UNCLASSIFIED NL

1 OF 1
AD A 103 307

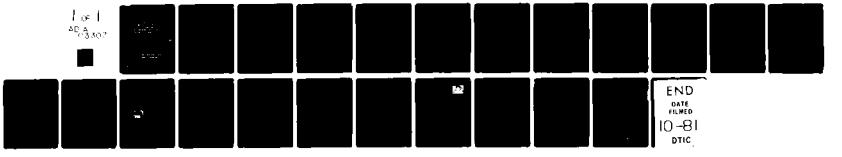

END
DATE FILMED
10-81
DTIC

AIAA-81-1244 Transonic Shock—Turbulent Boundary Layer Interaction and Incipient Separation on Curved Surfaces

G. R. Inger, University of Colorado, Boulder, CO; and

AIAA 14th Fluid and Plasma Dynamics Conference

June 23-25, 1981/Palo Alto, California

TRANSONIC SHOCK - TURBULENT BOUNDARY LAYER INTERACTION AND INCIPIENT SEPARATION ON CURVED SURFACES

George R. Inger*
University of Colorado
Boulder, Colorado

Abstract

A detailed analysis is made of weak normal shock - turbulent boundary layer interactions on longitudinally-curved surfaces for the case of non-separating steady 2-D flow. It is shown that the interactive viscous displacement effect on the local outer inviscid transonic flow eliminates the well-known singularity pertaining to a curved wall. The inner interaction solution within the boundary layer reveals that curvature moderately influences the interaction through the turbulent eddy viscosity. A non-asymptotic triple-deck solution valid over a wide range of practical Reynolds numbers is given which incorporates this effect, and example numerical results are presented and verified by comparison with experimental data. Small amounts of curvature ($K\delta_o \lesssim .01-.02$) are found to moderately spread out and thicken the interaction zone while also delaying slightly the onset of any incipient separation that occurs under the shock.

Nomenclature

a^*	Speed of sound at sonic conditions
C_f	Skin friction coefficient ($= 2\tau_w/\rho_{e_1} U_{e_1}^2$)
C_p	Pressure coefficient ($= 2p'/\rho_{e_1} U_{e_1}^2$)
F,G	Functions defined in Eqs. 20,23
h	Body shape function, see Fig. 7
H_i	Incompressible form factor ($= \delta_i^* / \theta_i^*$)
K	Wall curvature ($= 1/R_B$)
L	Distance to shock location
M	Mach number
p	Static pressure
p'	Interactive pressure perturbation ($= p - p_1$)
Δp	Pressure jump across incident shock
R_B	Wall radius of curvature ($\simeq K^{-1}$)
Re_ℓ	Reynolds number based on length ℓ
Re_L	Reynolds number ($= \rho_{e_1} U_{e_1} L / \mu_{e_1}$)
S,T	Transformed dependent variables, Eq. 17
T	Absolute temperature
u,v	Velocity components in x,y directions, respectively
u',v'	Streamwise and normal interactive disturbance velocity components, respectively
U_o	Undisturbed incoming boundary layer velocity in x-direction
W	Resultant flow velocity
x,y	Coordinates along and normal to body surface
X,Y,Z	Stretched independent variables, Eqs. 18,21
$y_{w_{eff}}$	Effective wall shift seen by interactive inviscid flow
β	Shock wave angle, Fig. 6
γ	Specific heat ratio
δ	Boundary layer thickness
δ^*	Boundary layer displacement thickness
ε_T	Kinematic turbulent eddy viscosity
η	Non-dimensional interactive displacement thickness
ϑ	Resultant flow direction angle
θ^*	Momentum thickness
μ	Ordinary coefficient of viscosity
ν	μ/ρ
ρ	Density
σ	Similarity parameter (see Eq. 18)
τ	Total shear stress
$\bar{T}$	Basic interactive wall-turbulence parameter
ω	Viscosity-temperature dependence exponent, $\mu \sim T^\omega$

Sub- and Superscripts

0	Undisturbed incoming boundary layer properties
1	Inviscid flow conditions ahead of shock
2	Inviscid flow conditions behind shock
e	Conditions at boundary layer edge
inv	Inviscid disturbance solution value
w	Conditions at wall surface
( )'	Denotes perturbation from "0" state

1. Introduction

An understanding of transonic shock - turbulent boundary layer interactions is important in the aerodynamic design of high-speed aircraft wings (both ordinary and circulation-controlled), turbine and cascade blades in turbomachinery, and air breathing engine inlets and diffusors. Since these applications often involve curved surfaces and since a singularity is associated with a normal shock on a curved surface in purely inviscid flow, the influence of wall curvature on transonic shock - boundary layer interaction is an important basic and practical question. Oswatitsch and Zierep[1] studied the related problem of normal shock impingement on a curved wall in a purely inviscid flow; they found that convex curvature introduces a logarithmic singularity in the wall pressure in the form of a sharp post-shock expansion (Fig. 1), and this phenomenon has indeed been observed in inviscid numerical solutions by Emmons[2], Jameson[3] and others. However, in real flows even at high Reynolds numbers, it is known that viscous smearing and upstream influence effects arise due to the thin boundary layer along the surface which profoundly influence the physics of the local interactive flow[4,5]. Consequently, in view of the well-known role often played by viscosity in eliminating singularities, one would expect the boundary layer to significantly alter and perhaps even eliminate this inviscid curvature-induced singularity. In the present paper, we address this issue for the case of a weak nearly-normal transonic shock interacting with a 2-D non-separating turbulent boundary layer. Our approach is to extend the successful transonic shock - boundary layer in-

*Professor and Chairman, Aerospace Engineering Sciences
Associate Fellow AIAA

teraction theory of Inger[6] to include the new features introduced by the combined inviscid and turbulent boundary layer flows on a curved wall.

Following brief overviews of the general physical features of the problem and the non-asymptotic triple-deck solution method in the flat surface case, we first made a detailed analysis of the local mixed transonic inviscid flow structure outside the boundary layer when it is interactively-coupled with the attendant thickness response of the layer. The results show that the inviscid singularity disappears (the external flow being now quite regular) when the boundary layer displacement effect is taken into account. We then examine the inner disturbance problem within the boundary layer, where it is shown that surface curvature does exert an influence on the interaction, but from a hitherto-overlooked source: its effect on the turbulent eddy viscosity. Using an approximate incorporation of this effect into the triple-deck solution, example numerical results are given and validated by experimental comparisons. A re-interpretation of curved wall data in the light of the present findings is also given along with parametric study results establishing the conditions for incipient separation on curved as well as flat surfaces.

2. Typical Features of the Interaction

As a background, consider the typical principal physical features of a non-separating normal shock - turbulent boundary layer interaction. To fix ideas, we consider an undisturbed turbulent boundary layer in the practical Reynolds number range $10^5 < Re_L < 10^8$ that is perturbed by a normal or nearly-normal shock weak enough to avoid separation ($M_1 \lesssim 1.3$); whether the wall is flat or curved, it is an experimental fact under these conditions that the resulting interaction flow pattern is of the relatively simple type illustrated in Fig. 2A. The boundary layer spreads out the shock perturbation upstream as well as downstream to give a wall pressure distribution such as shown in Fig. 2B, with a corresponding significant growth of the boundary layer displacement thickness particularly behind the shock, so that even though the original undisturbed boundary layer is thin and negligibly affects the overlying inviscid flow, this is no longer the case in the interaction zone astride the shock whether or not the wall is flat (Figs. 2B-E).

Thus, the local outer inviscid flow "sees" the overall viscous effects in the interaction as an effective thickening of the geometrical surface by an amount equal to the interactive displacement thickness growth. In the vicinity of the shock, this is seen to involve (a) a rapid growth in the effective body slope at the shock foot followed by (b) an overall downstream increase of the effective body thickness. At the very least, these two features must be included in any realistic mathematical model of the true outer inviscid flow in such interactions. Indeed, this conclusion is strongly supported by recent studies of interaction effects by Yoshihara[18] and Murman[19].

3. Non-Asymptotic Triple-Deck Treatment of Flat-Surface Interactions

3.1) Triple-Deck Structure

It is well-known experimentally that when separation occurs, the disturbance flow pattern associated with normal shock - boundary layer interaction is a very complicated one involving a bifurcated shock pattern[7], whereas the unseparated case pertaining to turbulent boundary layers up to $M_1 \lesssim 1.3$ has instead the much simpler type of interaction pattern (Fig. 2A) which is more amenable to analytical treatment. With some judicious simplifications, it is possible to construct a fundamentally-based approximate theory of this flow problem for flat walls. For purposes of orientation and completeness, a brief outline of the essential features of this theory will now be given (see Ref. 6 for full details).

Consider a known adiabatic boundary layer profile $M_o(y)$ subjected to small transonic disturbances due to an impinging weak and nearly normal shock. At high Reynolds numbers it has been established[8,10] that the resulting interactive perturbation field in the neighborhood of the shock organizes itself into three basic layers or "decks" (Fig. 3): (1) an outer region of potential inviscid flow above the boundary layer, containing the incident shock and interactive wave systems; (2) an intermediate deck of frozen shear stress-rotational inviscid disturbance flow occupying the outer 90% or more of the incoming boundary layer thickness; (3) an inner shear-disturbance sublayer adjacent to the wall which accounts for the interactive skin friction perturbations (and hence any possible incipient separation) plus most of the upstream influence of the interaction. The "forcing function" of the problem here is thus impressed by the outer deck upon the boundary layer; the middle deck couples this to the response of the inner deck but in so doing can itself modify the disturbance field, while the slow viscous flow in the thin inner deck reacts strongly to the pressure gradient disturbances imposed by these overlying decks. In the practical Reynolds number range of interest here, we analyze this disturbance field with a non-asymptotic triple-deck treatment patterned in many ways after Lighthill's approach[4] because of its essential soundness and adaptability to further improvement, its similarity to related multiple-deck approaches that have proven highly successful in treating turbulent boundary layer response to strong known adverse pressure gradients, and the large body of data that supports the predicted results in a variety of specific problems.

3.2) Formulation of the Disturbance Problem

Outer Potential Flow Region

If the incident shock and its reflection system are weak with isentropic non-hypersonic flow, we have a small disturbance potential inviscid motion in the undisturbed uniform flow U_{o_e}, M_{o_e}:

$$\frac{\partial^2 p'}{\partial y^2} + \left(1 - M_{o_e}^2 - 2\,\frac{u' M_{o_e}^2}{U_{o_e}}\right)\frac{\partial^2 p'}{\partial x^2} = 0 \qquad (1)$$

where the third term within the square brackets is significant in the transonic case $1 < M_{o_e} < 1.05\text{-}1.10$ and includes shock jump conditions to this order of approximation. Since various solution methods are available in either transonic or purely supersonic

flow (in which case Eq. 1 reduces to an Ackeret problem), we assume that such a solution may be carried out for all x on $y > \delta_o$ subject to the usual far-field conditions as $y \to \infty$. The remaining disturbance boundary condition along $y = \delta_o$ then couples this solution to the underlying double-deck: it requires that both v'/U_o and p' be continuous there.

Middle Rotational-Disturbance Flow Deck

This layer contributes to and transmits the displacement effect, contains the boundary layer lateral pressure gradient due to the interaction and carries the influence of the incoming boundary layer profile shape. Our analysis rests on the key simplifying assumption that for non-separating interactions the turbulent Reynolds shear stress changes are small enough to have a negligible back effect on the mean flow properties along the interaction zone; hence, they are "frozen" along each streamline at the appropriate value in the undisturbed incoming boundary layer. This approximation is well-supported by detailed experimental studies[11,12]. Thus the disturbance field is one of small rotational inviscid perturbation of the incoming non-uniform turbulent boundary layer profile governed by

$$\frac{\partial}{\partial y}\left[\frac{v'(x,y)}{U_o(y)}\right] = \left[\frac{1 - M_o^2(y)}{\gamma M_o^2(y)}\right] \frac{\partial(p'/p_o)}{\partial x} \qquad (2)$$

$$\frac{\partial^2 p'}{\partial y^2} - \frac{2}{M_o}\frac{dM_o}{dy}\frac{\partial p'}{\partial y} + (1 - M_o^2 - \frac{2u'M_o^2}{U_o})\frac{\partial^2 p'}{\partial x^2} = 0 \qquad (3)$$

where $U_o(y)$, $\rho_o(y)$ are arbitrary functions of y with δ_o, δ_o^* and τ_{w_o} as constants. Now Eq. 3 is a slight generalization of Lighthill's well-known pressure perturbation equation for non-uniform flows, which includes a non-linear correction term for transonic effects including the diffracted impinging shock above the sonic level of the incoming boundary layer profile. Excluding the hypersonic regime, Eqs. 2 and 3 therefore apply to a wide range of initially supersonic external flow conditions and across the boundary layer except at the singular point $M_o \to 0$ (which we avoid by consideration of the inner deck as shown below). Whatever the method used to solve this middle deck disturbance problem, we imagine that it provides the disturbance pressure distribution $p'(x,y)$; then y-integration of Eq. 2 gives the disturbance streamline slope as

$$\frac{v'(x,y)}{U_o(y)} = \underbrace{\frac{v'}{U_o}(x, y_{w_{eff}})}_{=0} + \frac{\partial}{\partial x}\left\{\int_{y_{w_{eff}}}^{y} \frac{p'}{\gamma p_{e_1}}\left[\frac{1 - M_o^2(\bar{y})}{M_o^2(\bar{y})}\right] d\bar{y}\right\} \qquad (4)$$

where $y_{w_{eff}} > 0$ is the effective wall height of the inner deck defined such that the inviscid $v'(x, y_{w_{eff}})$ and hence $\partial p'/\partial y(x, y_{w_{eff}})$ both vanish (see below).

The corresponding displacement thickness growth along the interaction is then given by streamwise-quadrature of the continuity equation integral as

$$\Delta\delta^*(x) \simeq \int_{y_{w_{eff}}(x)}^{\delta} \frac{p'}{p_{e_1}}\left[\frac{1 - M_o^2(\bar{y})}{M_o^2}\right] d\bar{y} + (\delta_o - \delta_o^*)\left[\frac{M_{e_1}^2 - 1}{M_{e_1}^2 p_{e_1}}\right] p_w'(x) \qquad (5)$$

The Inner Shear-Disturbance Layer

This thin inner deck contains the significant viscous and turbulent shear stress disturbances due to the interaction. It lies well within the Law of the Wall region of the incoming boundary layer and below the sonic level of the profile. The original work of Lighthill[4] and others further neglected the turbulent stresses and considered only the laminar sublayer effect; while this yields an elegant analytical solution, the results are in error at high Reynolds numbers and cannot explain the ultimate asymptotic behavior pertaining to the $Re_\ell \to \infty$ limit. The present theory remedies this by including the entire Law of the Wall region turbulent stress-effects. Note that our consideration of the entire Law of the Wall combined with the use of effective inviscid wall concept to the inner deck displacement effect eliminates the "blending layer"[3] that is otherwise required to match the disturbance field in the laminar sublayer region with the middle inviscid deck, since we impose a boundary condition of vanishing total shear disturbance at the outer edge of the deck.

To facilitate a tractable theory, we retain only the main physical effects by introducing the following simplifying assumptions: (1) the incoming boundary layer Law of the Wall region is characterized by a constant total (laminar plus turbulent eddy) shear stress and a Van Driest-Cebeci type of damped eddy viscosity model. (2) For weak incident shocks, the sublayer disturbances are small perturbations upon the incoming boundary layer; however, all the physically-important effects of streamwise pressure gradient, streamwise and vertical acceleration, and both laminar and turbulent disturbance stresses are retained. Moreover, since the form of the resulting set of linear equations is in fact unaltered by non-linear effects, the the quantitative accuracy is expected to be good until close to separation. (3) For adiabatic flows at low-to-moderate external Mach numbers, the undisturbed and perturbation flow Mach numbers are both quite small within the shear disturbance sublayer; consequently, the influence of the density perturbations may be neglected, while the corresponding compressibility effect on the undisturbed profile is treated by using incompressible relations based on wall recovery temperature properties. (4) The turbulent fluctuations and the small interaction disturbances are uncorrelated. (5) The thinness of the inner deck allows neglect of its lateral pressure gradient: $p' = p_w'(x)$.

Under these assumptions, the disturbance field is governed by the continuity and momentum equations

$$\frac{\partial u'}{\partial x} + \frac{\partial v'}{\partial y} = 0 \qquad (6)$$

$$U_o \frac{\partial u'}{\partial x} + v' \frac{dU_o}{dy} + (\rho_{w_o})^{-1} \frac{dp'_w}{dx} = \frac{\partial}{\partial y}\left(\nu_{w_o} \frac{\partial u'}{\partial y} + \epsilon_{T_o}' \frac{\partial u'}{\partial y} + \epsilon_T' \frac{dU_o}{dy}\right) \qquad (7)$$

where ϵ_T' is the kinematic eddy viscosity perturbation. The corresponding undisturbed turbulent boundary layer Law of the Wall profile $U_o(y)$ governed by

$$\tau_o(y) = \text{const.} = \tau_{w_o} = [\mu_{w_o} + \rho_{w_o} \epsilon_{T_o}(y)] \frac{dU_o}{dy} \qquad (8)$$

where the Van Driest-Cebeci eddy viscosity model with $y^* = \sqrt{\tau_{w_o} / \rho_{w_o}} / \nu_{w_o}$ yields for non-separating flow that

$$\epsilon_{T_o} = [.41y\,(1 - e^{-y^*/A})]^2 \frac{dU_o}{dy} \qquad (9a)$$

$$\epsilon_T' \simeq \left(\frac{\partial u' / \partial y}{dU_o / dy}\right) \epsilon_{T_o} \qquad (9b)$$

where we take the commonly-accepted value $A = 26$.

We seek to solve Eqs. 6-9 subject to the impermeable wall no-slip conditions $U_o(0) = u'(x,o) = v'(x,o) = 0$ plus an initial condition requiring all interactive disturbances to vanish far upstream. Furthermore, sufficiently far from the wall, u' must pass over to the inviscid solution u'_{inv} along the bottom of the middle deck governed by Eq 6 plus

$$U_o \frac{\partial u_{inv}}{\partial x} + v'_{inv} \frac{dU_o}{dy} + (\rho_{w_o})^{-1} \frac{\partial p_w}{\partial x} \simeq 0 \qquad (10)$$

while the corresponding total shear disturbance $(\partial u' / \partial y)$ vanishes to a desired accuracy.

Now differentiate Eq. 7 w.r.t. x, substitute Eq. 6 so as to eliminate u' and then differentiate the result w.r.t. y so as to eliminate p'_w; this yields the following fourth-order equation for v':

$$\frac{\partial}{\partial x}\left(U_o \frac{\partial^2 v'}{\partial y^2} - \frac{d^2 U_o}{dy^2} v'\right) = \frac{\partial^2}{\partial y^2}\left[(\nu_{o_w} + 2\,\epsilon_{T_o}) \frac{\partial^2 v'}{\partial y^2}\right] \qquad (11)$$

This equation contains a three-fold influence of the turbulent flow: the profile $U_o(y)$, its curvature d^2U_o / dy^2 (non-zero outside the laminar sublayer) and a new eddy disturbance stress term $2\,\epsilon_{T_o}$.

Eq. 11 is to be solved together with Eqs. 8,9 and the wall boundary conditions $v'(x,o) = \partial v' / \partial y(x,o) = 0$. A third condition involving v' is obtained by satisfying the x-momentum equation right at the wall:

$$\frac{\partial^3 v'}{\partial y^3}(x,o) = -(2\,\nu_{o_w})^{-1} \frac{d^2 p'_w}{dx^2} \qquad (12)$$

The fourth boundary condition is the outer inviscid matching from Eq. 10:

$$\frac{\partial}{\partial x}\left(U_o \frac{\partial^2 v'_{inv}}{\partial y^2} - v_{inv} \frac{d^2 U_o}{dy^2}\right) = 0 \qquad (13)$$

along with $\partial^2 v' / \partial y^2 \simeq 0$ (i.e., vanishing total disturbance shear). Once this $v'(x,y)$ field is obtained, the attendant streamwise velocity and hence the disturbance shear stress) may then be found from Eq. 6.

An important feature here is the "effective inviscid wall" position (or displacement thickness) that emerges from the asymptotic behavior of v' far from the wall[4] (Fig. 4A). This is defined by the value $y_{w_{eff}}$ where the "back projection" of the v_{inv} solution vanishes; physically, $y_{w_{eff}}$ thus represents the total mass defect height due to the shear stress perturbation field and hence the effective wall position seen by the overlying inviscid middle deck disturbance flow. As indicated in Fig. 4B, this couples the inner- and middle-deck solutions by providing the non-singular inner equivalent slip-flow boundary conditions

$$\partial p' / \partial y\,(y_{eff}) = v'_{inv}\,(y_{w_{eff}}) = 0 \text{ at } U_o\,(y_{w_{eff}}) > 0$$

for the middle-deck solution.

3.3) Approximate Solution by Operational Methods

An approximate analytic solution is further achieved by assuming small linearized disturbances ahead of and behind the nonlinear shock jump* plus an approximate treatment of the detailed shock structure within the boundary layer, which give accurate predictions for all the properties of engineering interest when $M > 1.05$. The resulting equations can be solved by operational methods[6,9] yielding the interactive pressure rise, displacement thickness growth and the skin friction behavior downstream and upstream of the shock foot. In particular, the matching of the outer two decks with the inner shear-disturbance deck in connection with the Fourier inversion process yields the determination of the upstream influence distance ℓ_u, the inner deck displacement thickness

$$\frac{y_{w_{eff}}}{\delta_o} = .677\left[\frac{C_{f_o}}{2} Re_{\delta_o}^2 \left(\frac{T_{e_o}}{T_w}\right)^{1+2\omega}\right]^{-1/3} (\kappa_{min}\delta_o)^{-1/3} H(T)\, P^{-1/3} \qquad (14)$$

and the interactive skin friction relation

$$\frac{\tau'_w(x)}{\tau_{w_o}} = -\left(\frac{\kappa_{min}}{\lambda}\right)^{2/3} S(T) \cdot \sqrt{\frac{\beta}{C_{f_o}}}\, C'_{p_w}\, P^{2/3} \qquad (15)$$

where

$$T \equiv (.41)^2 \left[\frac{C_{f_o}}{2} Re_{\delta_o} (T_{e_o}/T_w)^{1+2\omega}\right]^{1/3} \cdot (\kappa_{min}\delta_o)^{2/3} \qquad (16a)$$

*This nonlinear shock jump provision plus the various non-uniform viscous flow effects within the boundary layer reduces the lower Mach number limit otherwise pertaining to the linearized supersonic theory in purely inviscid potential uniform flow.

$$P \equiv \left[\frac{2(p_w')^{3/2}}{3\kappa_{min} \int_{-\infty}^{x} (p_w')^{3/2} dx} \right]^{2/3} \qquad (16b)$$

$$\lambda \delta_o \equiv .744 \beta^3 (C_{f_o}/2)^{5/4} \, Re_{\delta_o} / (T_{e_o}/T_w)^{\omega + 1/2} \qquad (16c)$$

where $\kappa_{min} = \ell_u^{-1}$ is given in Ref. 6 while the functions H(T) and S(T), shown here in Fig. 5, represent the wall turbulence effect on the interactive displacement effect and skin friction, respectively. Fig. 5 is a central result, providing a unified account of the entire Reynolds number range in terms of the single new turbulent interaction parameter T from the limiting behavior of negligible wall turbulence effect pertaining to the $T \to 0$ limit[4,9] to the opposite extreme of wall turbulence-dominated behavior at $T >> 1$ pertaining to an asymptotic-type of theory[8,10] at very large Reynolds numbers where the inner deck thickness and its disturbance field become vanishingly small.

A computer program has been constructed to carry out the foregoing solution method; it involves the middle-deck disturbance pressure solution coupled to the inner deck by means of the effective wall shift (Eq. 14) combined with an upstream influence solution subroutine. The corresponding local total interactive displacement thickness growth and skin friction are obtained from Eqs. 5 and 15, respectively. If desired, the attendant boundary layer shape factor change along the interaction may then also be calculated as $H = [\delta^*_o + \Delta\delta^*(x)]/\theta^*(x)$ with θ^* given by an x-wise integration of the overall momentum integral equation for the total local boundary layer since p(x), δ^* and C_f are known. The incoming turbulent boundary layer is treated by the compressible version of a universal composite Law of the Wall - Law of the Wake model due to Walz[13] that not only has a convenient analytical form (see Appendix) but also provides a very general fundamental description of this boundary layer in terms of three arbitrary parameters: preshock Mach number, boundary layer displacement thickness Reynolds number, and the incompressible shape factor H_{i_1}. This enables us to treat the important but heretofore-neglected influence of the upstream flow history (pressure gradient, suction, etc.) on the interaction; indeed, surface curvature effects on the pre-interactive flow may thus be taken into account also.

The aforementioned solution method captures all the essential global features of the mixed transonic viscous interaction flow, including lateral pressure gradient effects and interactive skin friction up to incipient separation for a very arbitrary input turbulent boundary layer profile. This has been verified by numerous detailed comparisons with experiment over a wide range of Mach - Reynolds number - shape factor conditions[14,16]. Thus the resulting predictions (such as typified by Fig. 2) are believed to give a sound engineering account of non-separating interaction regions in practical transonic flow fields and provide an appropriate framework for extension to the case of moderately-curved surfaces.

4. Extension to Curved Walls

Our analysis of the curved surface case is a composite treatment involving a basic hodograph analysis of the outer inviscid transonic flow due to Sobieczky[17] interactively linked to a wall curvature - corrected extension of the foregoing nonasymptotic triple-deck theory for the inner boundary layer region.

4.1) The Outer Inviscid Disturbance Flow

Consider the local mixed inviscid transonic flow in the neighborhood of the shock outside the boundary layer, assuming the shock weak enough to be isentropic. Then if W and ϑ are the magnitude and direction angle, respectively, of the resultant flow velocity and one introduces the transformed dependent variables

$$S = \pm \frac{3}{2} (\gamma+1)^{1/2} \, \sigma^{-1} \left(\frac{W}{a^*} - 1 \right)^{3/2} \qquad (17a)$$

$$t = \sigma^{-1} \vartheta \qquad (17b)$$

as functions of the stretched independent variables

$$X = x \qquad (18a)$$

$$Y = \frac{3}{2} (\gamma+1) \sigma^{1/3} y \qquad (18b)$$

where the constant σ is chosen later as an appropriate similarity parameter, then the governing transonic flow equations are:

$$S^{1/3} \frac{\partial S}{\partial X} - \frac{\partial t}{\partial Y} = 0 \qquad (19a)$$

$$S^{-1/3} \frac{\partial S}{\partial Y} + \frac{\partial t}{\partial X} = 0 \qquad (19b)$$

This pair of equations in general has either supersonic wave-type solutions ($S > 0$, minus sign in 19b) or subsonic Cauchy - Riemann - type solutions ($S < 0$, positive sign). If we further restrict attention to small perturbations about the shock condition, Eqs. 19 become linear in the leading approximation.

Now choose σ such that upstream of the shock $S = S_1 = 1$; then linearization of Eq. 19 gives a wave equation with solutions of the form[17]

$$S = S_1 + F_1(\xi) + G_1(\eta) \qquad (20a)$$

$$t = t_1 + F_1(\xi) - G_1(\eta) \qquad (20b)$$

where $\xi = X + Y$ and $\eta = X - Y$. Linearizing the subsonic equations for perturbations of the post-shock condition $S_2 < 0$, t_2 yields the following solution of the Cauchy-Riemann equations[17]:

$$Z = X + iS_2^{1/3} Y = S_2 + it_2 F_2(Z) \qquad (21)$$

A particular case of a pair of local solutions (Eqs. 20 and 21) pertains to the flow ahead of and behind an oblique shock of the "strong branch" type, i.e., with subsonic flow downstream. The

transonic shock jump conditions link the pre- and post-shock conditions as follows:

$$\Delta t = t_2 - t_1 = 2^{-3/2} \cdot 3 \cdot (1 - S_2^{2/3})^{1/2} (1 + S_2^{2/3}) \quad (22a)$$

$$\text{Ctg}\, \beta = 2^{-5/6} \cdot 3^{1/3} (\gamma + 1)^{1/3} \sigma^{1/3} (1 - S_2^{2/3})^{1/2} \quad (22b)$$

Thus, if at some point P there is a supersonic flow $W_1 > a^*$ at inclination ϑ_1 that is decelerated by an oblique shock to some $W_2 < a^*$ at angle ϑ_2 (Fig. 6A), then W_1, ϑ_1, W_2, ϑ_2 are related in terms of S_1, t_1, S_2, t_2 by means of Eqs. 17a, 17b, 22a. This is the transonic shock polar (Fig. 6B), and the wave angle β corresponding to the flow deflection angle* is found from Eq. 22b. Then with given shock jump conditions at P, the local solutions (Eqs. 20 and 21) may be used to determine the velocity gradients as well as the curvature of the shock shape in the vicinity of P.

This local transonic inviscid perturbation field now can be linked to the inner viscous disturbance flow by noting from above that the outer flow sees an effective body consisting of the bare wall $h_w = h_1 = C_1 X^2$ plus a slope jump C_2 at the shock foot followed by a further interactive displacement thickness growth, giving $h_2 = h_{w_{eff}} = C_2 X + D_2 X^2$ (see Fig. 7). Upstream of the shock, an arbitrary linear variation of inviscid flow Mach number along the wall is assumed to allow for either decelerating, accelerating or uniform incoming supersonic flow. Now in terms of this flow model, Sobieczky[17] carried out a local solution by means of a double series expansion analysis** of the upstream and downstream flow properties about the shock-foot origin using the following particular solutions of Eqs. 20 and 21:

$$F_1 = A_1 \xi \quad (23a)$$

$$G_1 = B_1 \eta \quad (23b)$$

$$F_2 = A_2 Z + B_2 Z \ln Z \quad (23c)$$

where the downstream (complex) coefficients A_2, B_2 are related to their upstream (real) counterparts and the shock shape parameters by the transonic shock polar. The results of this analysis yield two basically different types of physical behavior, one regular and the other singular, depending on whether the interactive deflection effect is included ($C_2 > 0$, $D_2 \neq C_1$) or neglected a priori ($C_2 = 0$, $D_2 = C_1$), as follows:

$C_2 > 0$, $D_2 \neq C_1$

REGULAR SOLUTION INCLUDING δ^*-EFFECT

Parabolic Oblique Shock Shape: $X_{sh} = Qy + Py^2$ (24a)

Linear Downstream Acceleration: $M_2 - 1 = K_2 + L_2 X$ (24b)

*It is assumed that the deflection angle $\vartheta_1 - \vartheta_2$ lies below the maximum value of the shock polar, which is reasonable in practice if the incident shock is weak enough to avoid separation.

**The realistic assumption is implied that the radius of any wall curvature is large compared with a typical boundary layer displacement thickness.

where this solution implies that the displacement thickness effect causes the inviscid shock to become curved near the boundary layer edge with a slightly oblique angle at the foot, as indeed observed experimentally[14,18-21] (see, e.g., Fig. 8).

$C_2 = 0$, $D_2 = C_1$

SINGULAR SOLUTION NEGLECTING δ^*-EFFECT

Curved Shock Normal to Wall: $X_{sh} = y^2 (Q + R \ln y)$ (25a)

Logarithmically Singular Shocked Flow:

$$M_2 = -K_1 (1 - E_2 X - F_2 X \ln X) \quad (25b)$$

In Eqs. 24 and 25 the parameters Q, P, K_2, L_2, R, K_1, E_2, F_2 are constant coefficients given in terms of C_1, C_2 and D_2 (see Ref. 17 for details). Now the "bare" curved wall solution (Eqs. 25) is in fact the *Oswatitsch-Zierep singular solution*[1] mentioned earlier. It has been of use mainly to verify computational results for inviscid flows with recompression shocks: fully-conservative codes for airfoils usually give results with sharp post-shock expansion on the curved suction surface, demonstrating the locally-exact treatment of the recompression shock if the computational grid is fine enough[3] — see Fig. 9. On the other hand, when the presence of the turbulent boundary layer is taken into account with its resulting ramp-like interactive displacement effect, the regular solution (Eqs. 24) is clearly the appropriate inviscid model even on a curved wall because it takes into account the flow deflection and oblique shock distortion due to this interaction-induced boundary layer thickening. This major conclusion has been forcefully corroborated by the supercritical airfoil flow field studies carried out by Murman et al[19]: as clearly illustrated in Fig. 10, when they include the influence of the interaction "bump" (modeled by a ramp similar to the one described here) on the effective inviscid solution wall shape, the post-shock singularity otherwise occurring on the curved surface completely disappears from their inviscid flow field calculations.

The foregoing discussion shows, at least for non-separating flows, that the interactive displacement thickness effect does indeed eliminate the inviscid singularity, giving in fact a well-behaved external inviscid disturbance flow. Moreover, it is seen that this regular influence of curvature on the inviscid flow via the displacement effect is necessarily of order δ^*/R_B and hence numerically very small in most practical applications. To be sure, wall curvature does have some influence, as shown below, but this is also quite regular and does not derive significantly from the inviscid part of the flow.

4.2) Inner Boundary Layer Region

Now wall curvature influences the inner solution in two ways: (1) it alters the incoming undisturbed turbulent boundary layer profile upon which the perturbation solution depends; (2) it introduces new explicit terms in the small disturbance equations. The first is by far the more important and is discussed further below; the secondary effects (2) are in fact negligible for the

small relative curvatures ($\delta_o/R_B \leq .02$) encountered in practice according to the following considerations. As regards the (regular) influence of curvature on the inviscid outer boundary conditions via the displacement effect, the foregoing analysis shows that this is of order δ_o^*/R_B and hence very small in the leading approximation. Likewise, under the continued assumptions that the interactive disturbances remain uncorrelated with the background turbulent fluctuation field and that the viscous disturbance sublayer lies within the Law of the Wall region of the turbulent boundary layer, the new terms in both the rotational inviscid and viscous disturbance sublayer equations can be shown to be of the same order or smaller and hence also negligibly small. Thus, to a consistent degree of first approximation, the form of the equations governing the disturbance flow in the boundary layer is not altered by wall curvature.

Regarding the basic turbulent flow profile, once again the explicit new curvature terms in the flow equations governing this profile (including the centrifugal lateral pressure gradient effect) have all been shown to be of the order δ_o/R_B and hence negligible (e.g., see Ref. 23 and more recent work[24]). However, the influence on the eddy viscosity relation is known to have an order of magnitude larger effect (10 to 20 times δ_o/R_B) on the overall skin friction and shape factor H_i; since it has been firmly established that the role of the profile in the interaction mainly derives from these properties[16,25], this influence is therefore deemed the cause of any significant curvature effect on the interaction solution.

By virtue of the foregoing arguments, the curvature effect can be reasonably estimated by incorporating into the incoming boundary layer profile model appropriate corrections for the influence of curvature on C_{f_o}, the shape factor and thickness. Examination of Bradshaw's comprehensive study[23] shows that over a wide range of parametric and local conditions, these corrections for small longitudinal curvature and non-separating flows can be adequately represented by the engineering approximations:

$$C_{f_o} \simeq \left(1 - 10\,\frac{\delta_o}{R_B}\right)\left(C_{f_o}\right)_{flat} \qquad (26a)$$

$$H_{i_1} \simeq \left(1 + 5\,\frac{\delta_o}{R_B}\right)\left(H_{i_1}\right)_{flat} \qquad (26b)$$

where to this first order accuracy the corresponding effect on δ_o is much smaller and therefore neglected. Note that the typical value $\delta_o/R_B \simeq .01$ yields a reduction and increase in C_{f_o} and H_{i_1} of 10% and 5%, respectively, which are an order of magnitude larger than the explicit new curvature terms in either the mean or perturbation flow equations (including the outer inviscid disturbances). The use of Eqs. 26 with δ_o/R_B as a fourth input parameter in the aforementioned non-asymptotic triple-deck theory thus enables a straightforward appraisal of the first order curvature effects on the non-separating normal shock - turbulent boundary layer interaction problem. In addition, this theory has been generalized[21,22] to include the influence of the shock obliquity (provided the post-shock state remains subsonic) which attends the displacment effect on the external inviscid flow.

5. Discussion of Results

5.1) Influence of Wall Curvature

A systematic study of the wall curvature effect based on the foregoing extended interaction theory has been made over a wide range of conditions for $K\delta_o = \delta_o/R_B$ ratios up to the largest values ($\leq .02$) normally found in practical applications. Representative results, which are representative of all the cases examined ($10^3 < Re\delta_o^* \leq 10^6$, $1.1 \leq M \leq 1.30$, $1.30 \leq H_{i_1} \leq 1.7$) are presented in Figs. 11 through 13 and will now be discussed.

The typical interactive pressure distributions presented in Figs. 11A and 11B show that wall curvature slightly spreads out the interaction, weakening the adverse pressure gradient, and that this effect derives primarily from the increased shape factor (Fig. 11A): The results for the pressure disturbance along the outer edge of the boundary layer (Fig. 11B) further bring out several interesting fundamental points. First, a small subsonic expansion region is predicted to occur right behind the shock regardless of the wall curvature; this is an inherent feature of the mixed transonic viscous interaction flow along a flat surface[9] as further confirmed by detailed numerical solutions[8] (Fig. 12) and Gadd's pipe flow experiments (Fig. 13). Thus, contrary to what is sometimes alleged, wall curvature per se is not the cause of such expansion regions in non-separating turbulent interactions. Second, when streamwise distance is properly rescaled so that $x \sim 0$ (δ_o) as is done in Fig. 11B, these regions are perfectly regular as predicted by Eqs. 24. Third, although not the cause, convex wall curvature does strengthen the expansion and reduce the preceding local shock pressure jump. We re-emphasize, however, that this is a result of the curvature effect on the boundary layer eddy viscosity and has nothing whatsoever to do with any inviscid curvature singularity.

Figs. 14A-D illustrate as a group the modest curvature effects on all the main streamwise properties along an interaction for a set of conditions quite typical of a full scale wing. Since curvature increases H_i and hence reduces the incoming profile "fullness," it acts to spread out the wall pressure disturbance, increase the upstream influence, reduce the downstream pressure level and (Fig. 14C) thicken the downstream boundary layer. The corresponding influence on skin friction (Fig. 14D) is also noteworthy: although curvature reduces the upstream level, it slightly increases the local C_f near the shock foot owing to the reduced adverse interactive pressure gradient and hence delays the onset of separation. This prediction is concordant with Gadd's assertion (p. 32 of Ref. 26) that "there is some direct evidence that curvature affects the way in which boundary layer velocity profiles respond to the rise of pressure... ; ... by convex surface curvature . . . thus separation might be delayed."

5.2) Comparisons with Experiment

Ackeret, Feldmann and Rott's famed experimen-

tal study[7] of shock - boundary layer interaction on a plate and wall in the choked transonic flow of a slightly-curved wind tunnel nozzle provides some examples of unseparated turbulent flow suitable for at least approximate comparison with the present theory. We have chosen those for which both wall and inviscid pressure distributions, as well as displacement thickness, are given. It should be noted, however, that direct comparisons with these data involve numerous uncertainties in converting to the theoretical variables (or vice-versa): (a) the boundary layer thickness and hence the inviscid flow edge is only approximately defined; (b) the shock wave location and shape are uncertain to within .25 δ_o to .50 δ_o; (c) reading the curves where they change rapidly introduces inherent error; (d) a significant background inviscid pressure gradient is present which beclouds interpretation of the outer fringes of the interaction zone and the character of the incoming "undisturbed" turbulent layer profile; (e) the upstream boundary layer history is only partially understood, especially following forced transition cases, and this together with (d) cannot be fully accounted for in the local interaction model; (f) some amount of channel blockage effect occurs from the interactive boundary layer thickening, which reduces the post-shock channel area and hence the effective theoretical shock strength and downstream interaction pressure level (this was independently identified by both Panaras and Inger[25] and Melnick and Grossman[27] who devised different but equivalent correction methods for it). For these reasons it is understood that the following comparisons are primarily of qualitative value.

A typical non-separating interactive pressure field measured by AF & R is illustrated in Fig. 15A; experimental pressure distributions along both the surface and the approximate boundary layer edge are compared in Fig. 15B with our theoretical prediction (corrected for the estimated interactive blockage effect* using the Panaras-Inger[25] method), while the corresponding displacement thickness and skin friction distributions are shown in Figs. 15C and 15D, respectively. We note that the relevant non-dimensional curvature parameter for these experiments was rather small ($K\,\delta_o \approx .0063$) so that the predicted curvature effect on the interaction is only slight, as indicated. Regarding the skin friction comparison shown in Fig. 15D, we note that the "experimental" values were actually inferred from measured velocity profiles along the interaction (hence θ^* and δ^*) by means of the 2-D momentum integral equation; considering the uncertainties of the experimental set up and this method, combined with the present theory's own limitations , the agreement is considered good as regards both the magnitude and shape of the C_f curve. Indeed, in view of the aforementioned difficulties in interpreting the data plus the approximations of the present small disturbance theory, the overall agreement is deemed to be quite good. In particular, the following definitive features of the interaction predicted by the the theory are well-corroborated: (1) the magnitude, sign and streamwise extent of the lateral pressure gradient effect both ahead of and behind the shock; (2) the existence of a long slow interactive pressure rise (algebraic rather than exponential) downstream of the shock; (3) the overall streamwise scale and upstream influence distance; (4) the magnitude and shape of the interactive displacement thickness growth; (5) the local inviscid pressure jump across the shock at the boundary layer edge; (6) a non-singular inviscid subsonic expansion region behind the shock due to the viscous-inviscid interaction and not surface curvature (note that the zero curvature in this region is actually closer to the data), consistent with the regular inviscid post-shock model.

A second set of comparisons, illustrated in Fig. 16, involves some recent DFVLR-AVA(Gö) data obtained on two supercritical airfoils with non-separating interaction zones on the curved upper surfaces. Here, the theoretical prediction method used incorporates the present analysis as a local interactive module within a global viscous-inviscid prediction program for supercritical airfoils[22]. It is seen that the theory yields predictions of both the wall pressure and displacement thickness distributions along the interaction region that are in excellent agreement with the measured values (indeed this was found true in many other cases not shown here[28]). Good agreement is also shown in the corresponding local skin friction behavior, where we note that the experimental C_f values were inferred from various streamwise station boundary layer profile surveys by means of the Ludwig Tillman relationship

$$C_f = .246(T^*/T_e)^{.796}\, Re_{\theta}{}^{*-.268}\, e^{-1.561\, H_i} \qquad (27)$$

where $T^*/T_e \approx 1 + .14\, M_e{}^2$ for $\gamma = 1.40$ and $P_r = .7$ on an adiabatic wall.

5.3) Incipient Separation

The particular attention paid by the present theory to the accurate analysis of local interactive skin friction behavior, including the role of wall curvature, makes it possible to establish conditions under which incipient separation ($C_{f_{local}} \to 0$) occurs. Thus setting $\tau_w = \tau_{w_o} + \tau_w' = 0$, Eq. 12 yields the following explicit analytical criterion for the onset of separation:

$$C'_{p_w}\left[\frac{2\, C'_{p_w}{}^{3/2}/\kappa_{min}}{3\int_{-\infty}^{x}(C'_{p_w})^{3/2}dx}\right]^{2/3} \geq \frac{\sqrt{C_{f_o}/\beta}}{S(T)}\left(\frac{\lambda}{\kappa_{min}}\right)^{2/3} \qquad (28)$$

where it is re-emphasized that C'_{p_w} here is the local interactive distribution. Eq. 28 bears a general resemblance to a Stratford-type[29] of incipient separation relation for turbulent flow, except that the present formula contains the integrated history effect along the interaction whereas Stratford's result involves purely local properties of C_{p_w} and dC_{p_w}/dx. It is understood, of course, that the present theory actually breaks down approaching such separation owing to the combination of its

*For the significant δ^* - increases (100-200%) typically encountered even in non-separating interactions, this blockage effect is found to be significant when all the wall surfaces are taken into account; in particular, for the relatively narrow channel dimensions of the AF & R tests, this method indicates that $\Delta P_{eff} \approx .825 \times \Delta P_{Rankine\text{-}Hugoniot}$

linearization assumptions and the Van Driest/Cebeci wall turbulence model used; nevertheless, Eq. 28 does give at least an approximate indication of where this will occur and indeed does so without containing any adjustable empirical constants. Note that according to the present theory wall curvature effects on incipient separation are implicitly accounted for via their influence on the values of C_{f_o} and H_{i_1} used in evaluating Eq. 28.

Based on the foregoing, a systematic parametric study of the critical shock strength for incipient separation vs. Reynolds number, shape factor and degree of wall curvature was carried out to establish a fundamental "incipient separation curve"; the results are shown in Fig. 17. Also indicated is the approximate experimental boundary determined by a careful examination of all available transonic interaction data[30], plus Nussdorfer's[31] well-known $M_1 \approx 1.30$ criterion for turbulent flow. It is seen that the theoretical prediction of a gradual increase in the $M_{1_{incip.sep.}}$ value with Reynolds number is in agreement with the experimental trend; moreover, the theoretical prediction of only a small influence of shape factor on the incipient separation conditions is also borne out by the lack of any consistent H-effect for the same Re discernible in the data. Stanewsky[28] and Squire[32] have experimentally observed similar insensitivities to H_{i_1} in transonic and purely supersonic flow interactions, respectively. The absolute values of $M_{1_{incip.sep.}}$ predicted by the present interaction theory are seen to be consistently slightly lower than the average experimental value; this is attributable to the combined effects of the linearized inner deck theory (which overpredicts the pressure gradient effect on C_f and hence too small an incipient separation shock strength) and the assumption of a normal shock when in fact most experiments likely entail some shock obliquity (which also delays separation to somewhat higher shock-strengths). In conjunction with these results it is interesting to note that Nussdorfer's original incipient separation criterion, based as it was on a very limited base, does roughly go through the average of the data although it does not account for the proper Reynolds number effect.

As shown in Fig. 17B, wall curvature in the range $0 \leq K\delta_o \leq .02$ has only a small effect on incipient separation: at Reynolds numbers below about $Re_L \sim 5 \times 10^7$, it delays the onset of separation to slightly higher shock strength for a given H_{i_1} owing to the reduced interactive pressure gradient that lowers $C_{f_{min}}$ (see Fig. 7), whereas at high Reynolds numbers the effect reverses sign owing to the eventual dominating influence on the curvature solution of the reduction in C_{f_o} with increasing Re_L. Qualitatively, therefore, the influence of curvature is similar to (but even smaller than) that of increasing shape factor (see Fig. 17A). Indeed, from a practical standpoint, the predicted curvature effect clearly lies within the indicated uncertainty band of the data establishing incipient separation.

6. Concluding Remarks

This investigation has sought to delineate the essential influence of surface curvature on non-separating turbulent boundary layer - transonic shock interactions, to place in true perspective the inviscid curvature singularity, and to devise an approximate analysis including curvature that enables parametric study, comparisons with experiment and an approximate prediction of incipient separation. The resulting theory is an approximate non-asymptotic triple deck model of the interaction pertaining to the Reynolds number range $10^5 \leq Re_L \leq 10^8$.

The major results of the study are the following. (1) When the viscous displacement effect on the inviscid flow is accounted for (as it should by very definition of an interaction problem), the surface curvature effect on non-separating interactions is non-singular, moderate and derives from its influence on the eddy viscosity within the boundary layer. (2) The region of sharp pressure rise followed by expansion observed along the edge of the boundary layer may be physically interpreted as inherent features of the viscous mixed transonic interaction that occur even on a flat surface and which are only secondarily-influenced by wall curvature. (3) Owing to the slight spreading out and hence weakening of the adverse interactive pressure gradient it causes, wall curvature delays the onset of incipient separation to slightly higher shock Mach numbers; for ordinary practical cases ($K\delta_o \lesssim .02$), however, this effect may be neglected.

Three areas of future application warranting further study appear to be of practical interest. (a) Extension of the present interaction theory to the unsteady case (examining first the validity of the quasi-steady approximation) in order to study unsteady air loads due to flutter at transonic speeds. (b) Adaptation to three dimensional flow fields of finite-span wings, at least outside wing/fuselage juncture or tip - influence regions. (c) More detailed study of the effects of shock - boundary layer interactions on transonic internal flows within engine inlets and ducts and turbomachinery blade passages and cascades. The influence of these interactions on the resulting losses and downstream effects, especially with incipient separation, is important to understand and predict in practice.

Acknowledgments

The author expresses a sincere appreciation to Dr. Robert Whitehead of the Office of Naval Research for his support of this work under Research Contract N00014-80-C-0470. A further note of gratitude is extended to Dr. Helmuth Sobieczky for many helpful discussions. Finally, the assistance of Mr. A. Deane with the numerical aspects of the work is acknowledged.

References

1. Oswatitsch, K., and J. Zierep, "Das Problem des Senkrechten Stosses an einer Gekrümmten Wand," ZAMM 40 (1960), p. 143.

2. Emmons, H. W., "Theoretical Flow of a Frictionless Adiabatic Perfect Gas Inside a Two-Dimensional Hyperbolic Nozzle," NACA TN-1003, 1946.

3. Jameson, A., "Iterative Solution of Transonic Flows Over Airfoils and Wings," Comm. Pure Appl. Math., Vol. 27, 1974, pp. 283-309.

4. Lighthill, M. J., "On Boundary Layers and Upstream Influence, II. Supersonic Flow Without Separation," Proc. Royal Soc. A 217, 1953, pp. 478-507.

5. Stewartson, K., and P. G. Williams, "Self-Induced Separation," Proc. Royal Soc. A 312, 1969, pp. 181-206.

6. Inger, G. R., "Upstream Influence and Skin Friction in Non-Separating Shock - Turbulent Boundary Layer Interactions," AIAA Paper 80-1411, Snowmass, Colorado, July 1980.

7. Ackeret, J., F. Feldman and N. Rott, "Investigation of Compression Shocks and Boundary Layers in Gases Moving at High Speed," NACA TN-1113, 1947.

8. Melnick, R. E., and B. Grossman, "Analysis of the Interaction of a Weak Normal Shock Wave With a Turbulent Layer," AIAA Paper 74-598, June 1974.

9. Inger, G. R., and W. H. Mason, "Analytical Theory of Transonic Normal Shock - Boundary Layer Interaction," (Abbreviated version published in AIAA Jour. 14, Sept. 1976, pp. 1266-1272.) Also AIAA Paper 75-831, June 1975.

10. Adamson, T. C., and A. Feo, "Interaction Between a Shock Wave and a Turbulent Layer in Transonic Flow," SIAM Jour. Appl. Math 29, July 1975, pp. 121-144.

11. Rose, W. C., and D. A. Johnson, "Turbulence in Shock Wave - Boundary Layer Interactions," AIAA Jour. 13, July 1975, pp. 884-889.

12. Rose, W. C., and M. E. Childs, "Reynolds Shear Stress Measurements in a Compressible Boundary Layer Within a Shock Wave - Induced Adverse Pressure Gradient," JFM 65, 1, 1974, pp. 177-188.

13. Walz, A., "Boundary Layers of Flow and Temperature," M.I.T. Press, Cambridge, Mass., 1969, p. 113.

14. Inger, G. R., "Analysis of Transonic Normal Shock - Boundary Layer Interaction and Comparisons With Experiment," AIAA Paper 76-331, July 1976 (VPI&SU Report Aero-053, Blacksburg, Va., Aug. 1976).

15. Inger, G. R., "Transonic Shock - Turbulent Boundary Layer Interaction with Suction or Blowing," AIAA Paper 79-0005, New Orleans, La., Jan. 1979. (Also see Jour. of Aircraft 15, Nov. 1978, pp. 750-754.)

16. Inger, G. R., "Some Features of a Shock - Turbulent Boundary Layer Interaction Theory in Transonic Flow Field," Proc. AGARD Symposium on Computation of Viscous-Inviscid Interactions, pp. 18-1 to 18-66, Colorado Springs, Colo., Sept. 1980.

17. Sobieczky, H., "A Computer Program for Analysis of Transonic Flows Past a Wall Ramp," Engineering Experiment Station, College of Engineering, The University of Arizona, Tucson, June 1978.

18. Yoshihara, H., and D. Zonars, "An Analysis of Pressure Distributions on Planar Supercritical Profiles," General Dynamics ERR-1684, San Diego, Calif., Dec. 1971.

19. Jau, W. H., and E. Murman, "A Phenomenological Model for Displacement Thickness Effects of Transonic Shock Wave - Boundary Layer Interactions," Paper 15-1, AGARD Conference on Viscous-Inviscid Interactions," Colorado Springs, Colo., Sept. 1980.

20. Sobieczky, H., and E. Stanewsky, "The Design of Transonic Airfoils with Consideration of Shock Wave - Boundary Layer Interaction," ICAS Paper 76-14, 1976.

21. Inger, G. R., and H. Sobieczky, "Shock Obliquity Effect on Transonic Shock - Boundary Layer Interaction," ZAMM 58T, 1978.

22. Nandanan, M., E. Stanewsky and G. R. Inger, "A Computational Procedure for Transonic Airfoil Flow Including a Special Solution for Shock - Boundary Layer Interaction," AIAA Paper 80-1389, Snowmass, Colo., July 1980.

23. Bradshaw, P., "Effects of Streamline Curvature on Turbulent Flow," Agardograph 169, Aug. 1973.

24. So, R. M., and G. L. Mellor, "Turbulent Boundary Layers with Large Streamline Curvature Effects," ZAMP 29, 1978, pp. 54-74.

25. Panaras, A. G., and G. R. Inger, "Transonic Normal Shock - Turbulent Boundary Layer Interaction in Pressure Gradient Flows," ASME Paper 77-GT-34, March 1977.

26. Gadd, G. E., "Interactions Between Normal Shock Waves and Turbulent Boundary Layers," British ARC 22559, R&M 3262, 1962.

27. Melnick, R.E., and B. Grossman, "Further Developments in an Analysis of the Interaction of a Weak Normal Shock Wave with a Turbulent Boundary Layer," Symposium Transonicum II, Springer-Verlag, 1975, pp. 262-272.

28. Stanewsky, E. (DFVLR-AVA Gö), Private communication.

29. Stratford, B. S., "The Prediction of Separation of the Turbulent Boundary Layer," Jour. Fluid Mech. 5, pp. 1-16, 1959.

30. Deane, A., "Reynolds Number and Shape Factor Effects on Transonic Shock - Turbulent Boundary Layer Interactions Including Incipient Separation," M. S. Thesis, Dept. of Aerospace Engineering, VPI&SU, Blacksburg, Va., Dec. 1980.

31. Nussdorfer, T. J., "Some Observations of Shock-Induced Turbulent Separation on Supersonic Diffusors," NACA RM E51L26, May 1956.

32. Squire, L. C., and M. J. Smith, "Interaction of a Shock Wave With a Turbulent Boundary Layer Disturbed by Suction," Aeronautical Quarterly (to be published).

33. Tai, T. C., "Theoretical Calculation of Viscous-Inviscid Transonic Flows," DWTNSRDC Report 80/104, Bethesda, Md., Aug. 1980.

Appendix

Because of its convenient analytical form, accurate blended representation representation of the combined Law of the Wall - Law of the Wake behavior and generality, we have adopted Walz's model for the incoming turbulent boundary layer upstream of the interaction. For the low Mach number adiabatic wall conditions appropriate to transonic interactions, it may be satisfactorily corrected for compressibility effects by the Eckert Reference Temperature method which under these conditions is, in fact, comparable in accuracy to, but far simpler to implement than, the Van Driest compressibility transformation approach.

Let π be Coles' (incompressible) Wake Function, $\eta \equiv y/\delta$ and denote for convenience $R = .41\, Re\delta_o^*/[(1+\pi)\,(T_w/T_e)^{1+w}]$, $T_w/T_e \simeq 1 + .18\,M_e^2$ with $w \simeq .76$ for a perfect gas; then the compressible form of Walz's composite profile may be written

$$\frac{U_o}{U_e} = 1 + \frac{1}{.41}\sqrt{\frac{C_{f_o}}{2}\left(\frac{T_w}{T_e}\right)}\left[\left(\frac{R}{1+R}\right)\eta^2(1-\eta) - 2\pi + 2\pi\,\eta^2\,(3-2\eta) + \ell n\left(\frac{1+R\eta}{1+R}\right) - (.215+.655R\eta)e^{-3R\eta}\right] \tag{A-1}$$

subject to the following condition linking π to C_{f_o} and $Re\delta_o^*$:

$$2\pi + .215 + \ell n(1+R) = \frac{.41}{\sqrt{\frac{C_{f_o}}{2}\left(\frac{T_w}{T_e}\right)}} \tag{A-2}$$

Eqs. (A-1) and (A-2) have the following desirable properties: (a) for $\eta \geq .10$ or so U_o/U_e is dominated by a Law of the Wake behavior which correctly satisfies both the outer limit conditions $U_o/U_e \to 1$ and $dU_o/dy \to 0$ as $\eta \to 1$; (b) on the other hand, for very small η values, U_o assumes a Law of the Wall - type behavior consisting of a logarithmic term that is exponentially damped out extremely close to the wall into a linear laminar sublayer profile $U/U_e \simeq R\eta$ as $\eta \to 0$; (c) Eq. (A-1) may be differentiated w.r.t. η to yield an analytical expression for dU_o/dy also, which proves advantageous in solving the middle and inner deck interaction problems (see text) where dM_o/dy must be known and vanish at the boundary layer edge.

The use of the incompressible form of Eq. (A-1) in the defining integral relations for δ_i^* and θ_i^* yields the following relationship that links the wake parameter to the resulting incompressible shape factor $H_{i_1} = (\delta_i^*/\theta_i^*)_1$:

$$\frac{H_{1_i} - 1}{H_{1_i}} = \frac{2}{.41}\sqrt{\left(\frac{T_w}{T_e}\right)\frac{C_{f_o}}{2}}\left(\frac{1 + 1.59\pi + .75\pi^2}{1+\pi}\right) \tag{A-3}$$

Eqs. (A-2) and (A-3) together with the defining relation for R enable a rather general and convenient parameterization of the profile (and hence the interaction that depends on it) in terms of three important physical quantities: the shock strength (M_e), the displacement thickness Reynolds number Re_{δ^*} and the shape factor H_{i_1} that reflects the prior upstream history of the incoming boundary layer including possible pressure gradient and surface mass transfer effects. With these parameters prescribed, the aforementioned three equations may be solved simultaneously for the attendant skin friction C_{f_o}, the value of R and, if desired, the π value appropriate to these flow conditions.

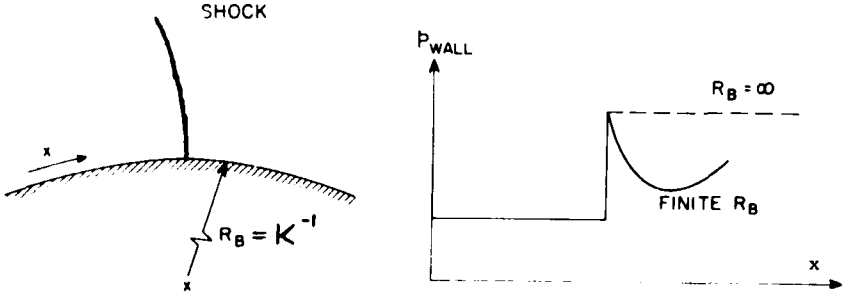

Fig. 1 Inviscid Shock-Flow on a Curved Wall

Fig. 2

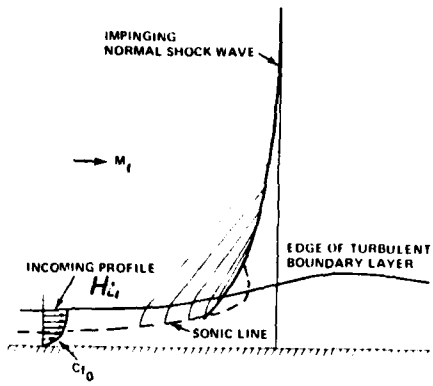

(a) Non-Separating Interaction Pattern

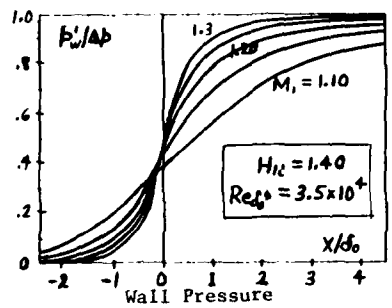

Wall Pressure

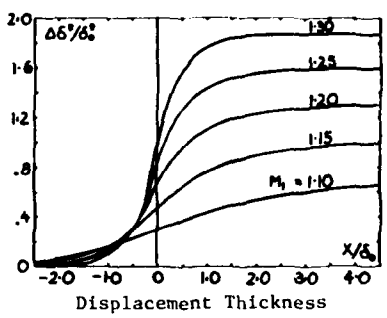

Displacement Thickness

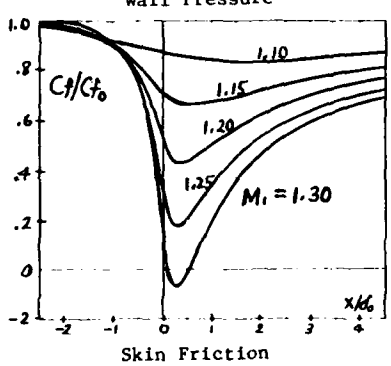

Skin Friction

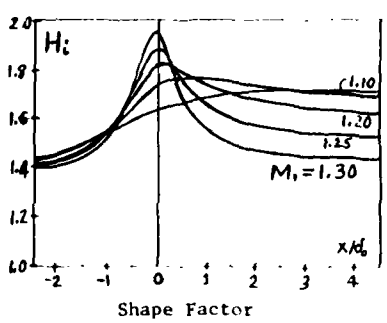

Shape Factor

(b) Typical Interaction Zone Properties

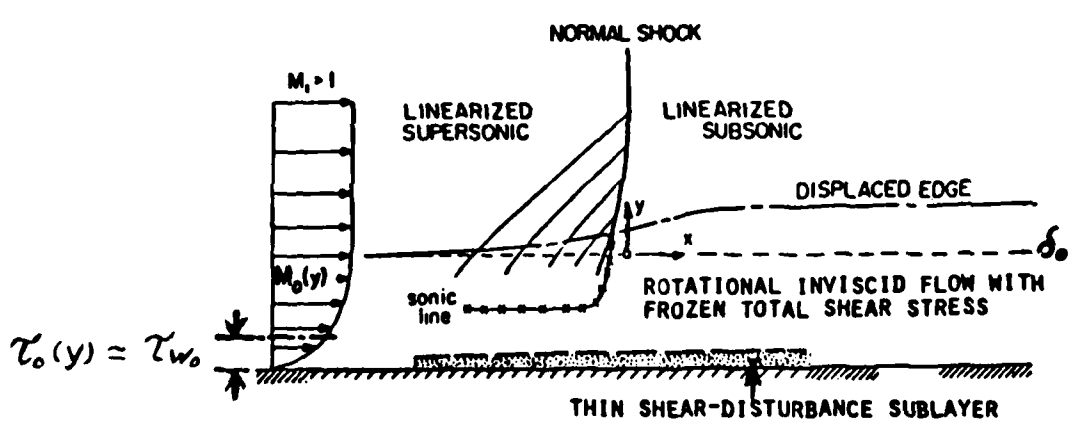

Fig. 3 Triple-Deck Structure of Interaction Field (Schematic)

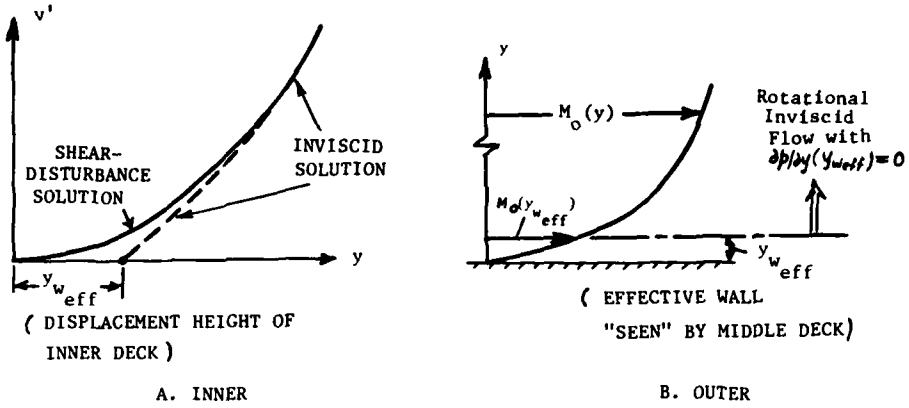

Fig. 4 Inner-Middle Deck Matching by the Effective Wall Concept

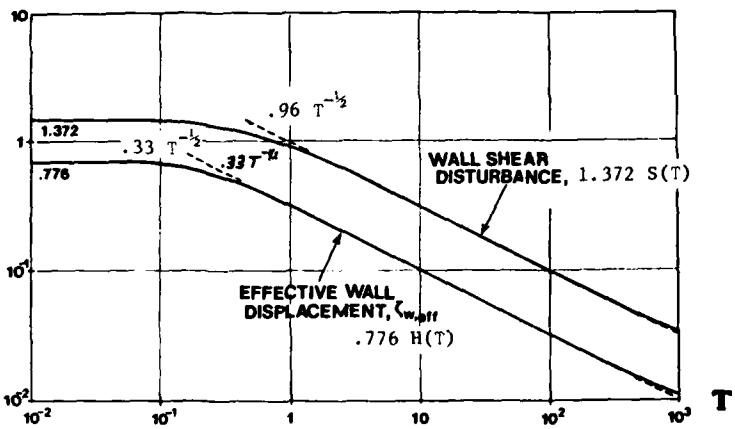

Fig. 5

Shear-Disturbance Sublayer Solution Properties

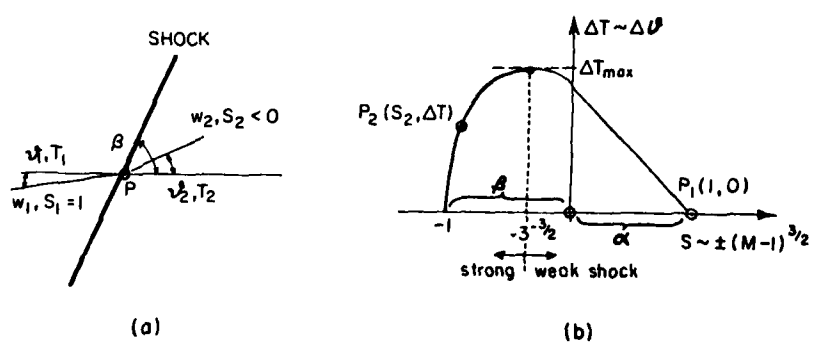

Fig. 6 Transonic Hodograph Variables and Shock Polar

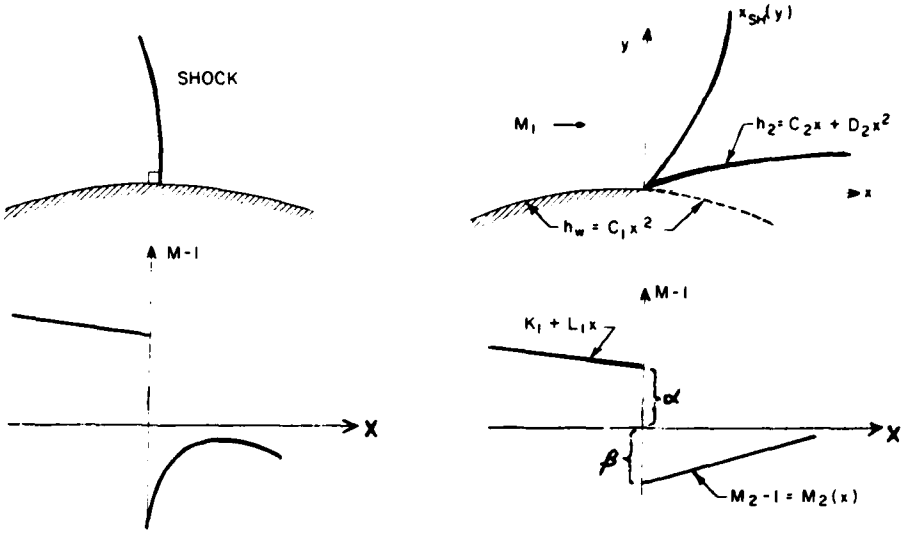

A. Singular: Viscous Displacement Effect Neglected.

B. Regular: Viscous Displacement Effect Included.

Fig. 7 Two Possible Inviscid Solutions for Outer Interactive Disturbance Flow[17]

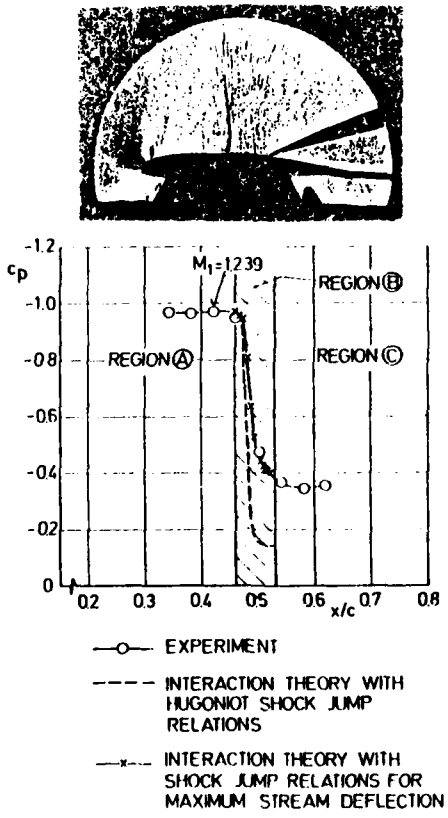

Fig. 8 Shock Obliquity due to Viscous Interaction[22]

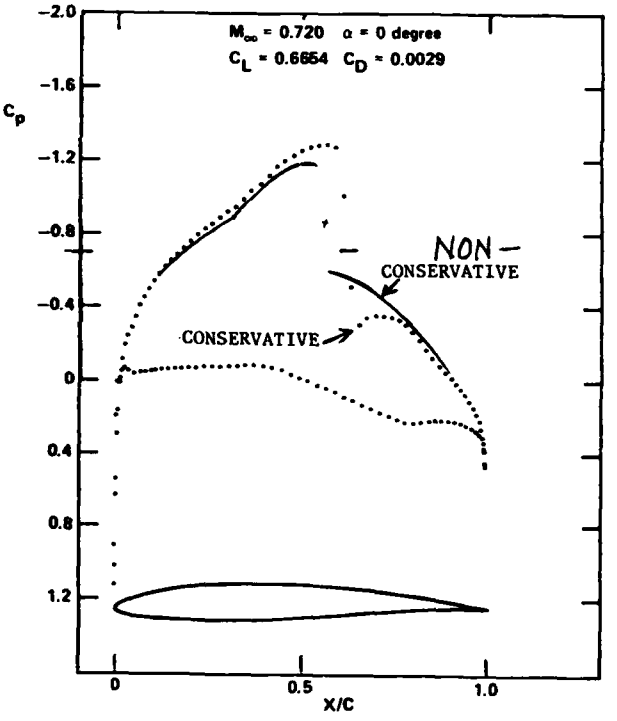

Fig. 9

Inviscid Post-Shock Singularity in Supercritical Airfoil Flow Field Calculations by Finite Difference Methods[33]

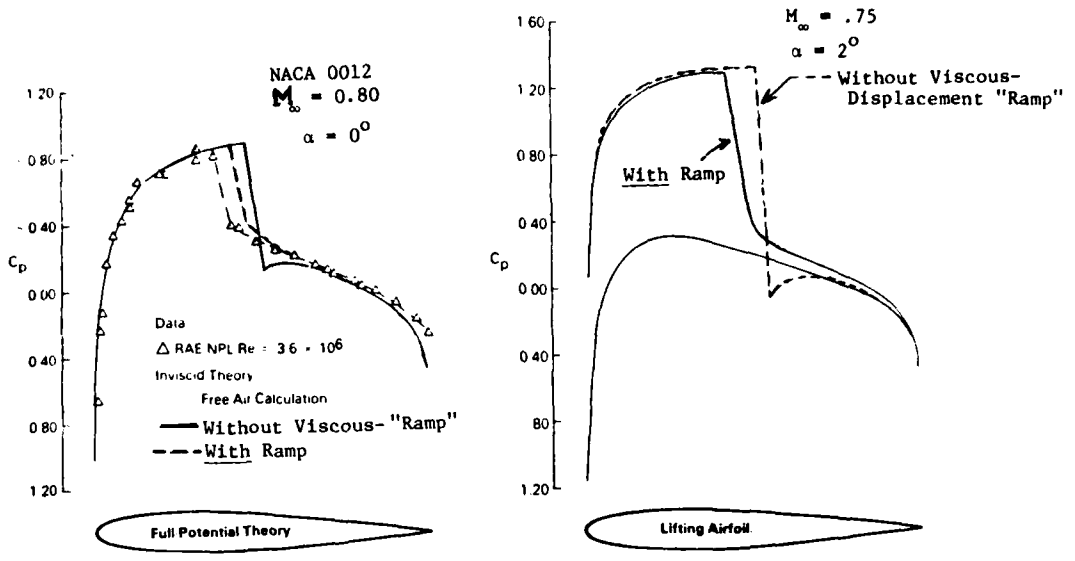

Fig. 10 Removal of Post-Shock Curvature Singularity by the Interactive Displacement Effect: Supercritical Airfoil Flow Field Calculations[19]

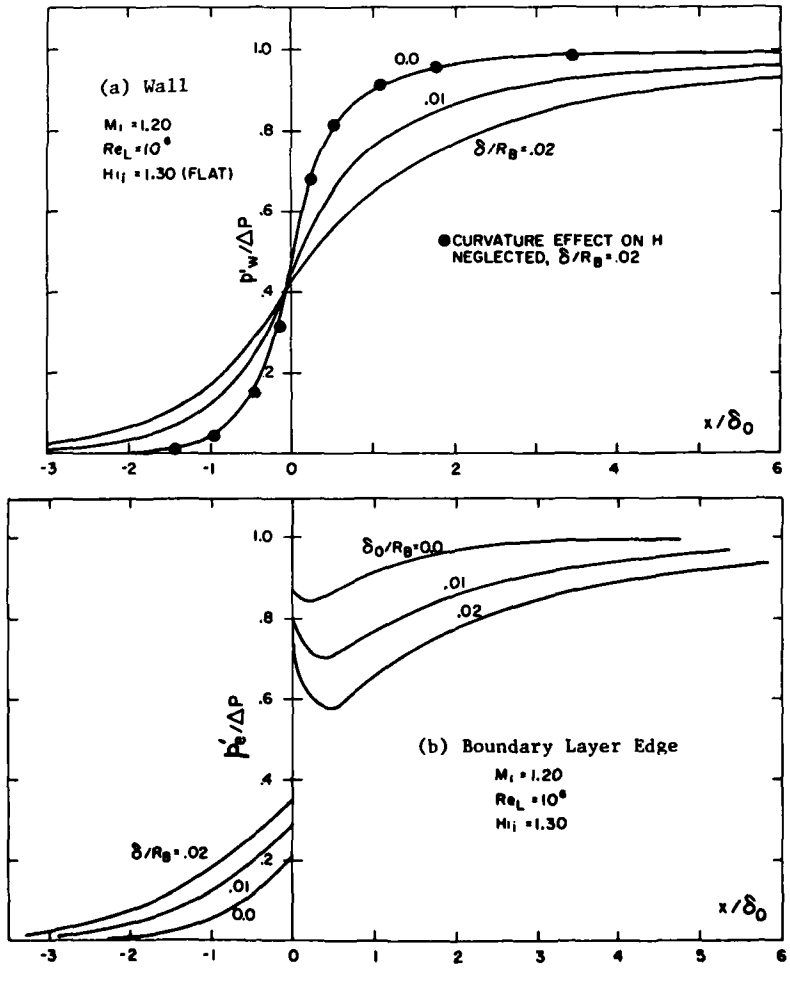

Fig. 11

Curvature Effect on Interactive Pressure Distributions

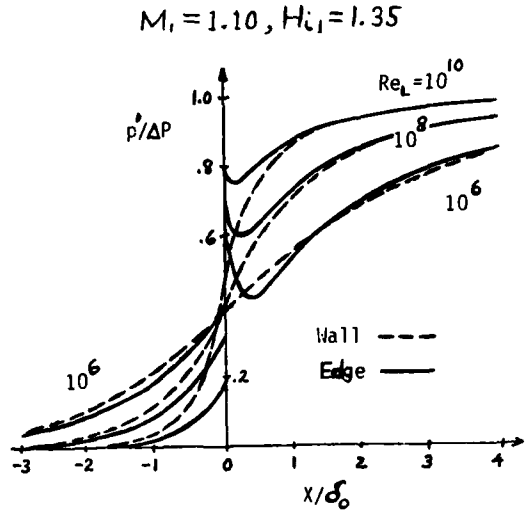

(a) Inger and Mason[9]

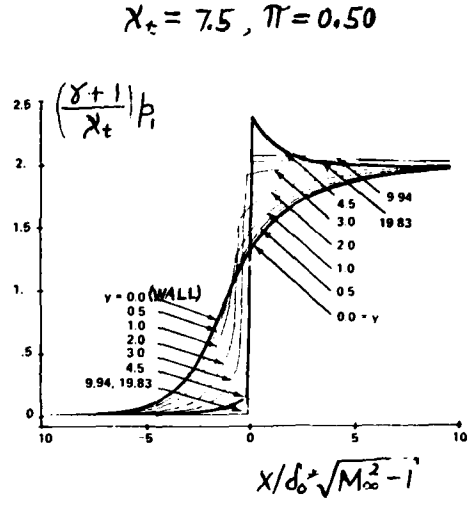

(b) Melnick and Grossman[8]

Fig. 12 Theoretical Interactive Pressure Distributions Along a Flat Surface

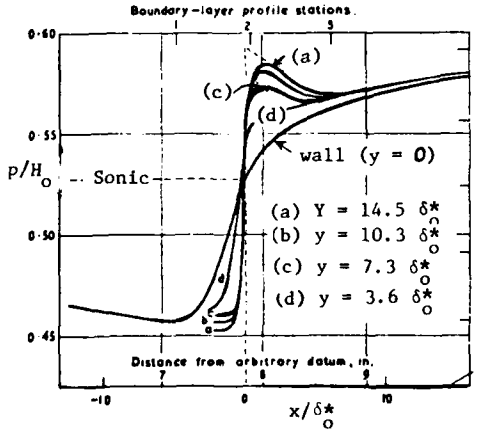

(a) Gadd[26]

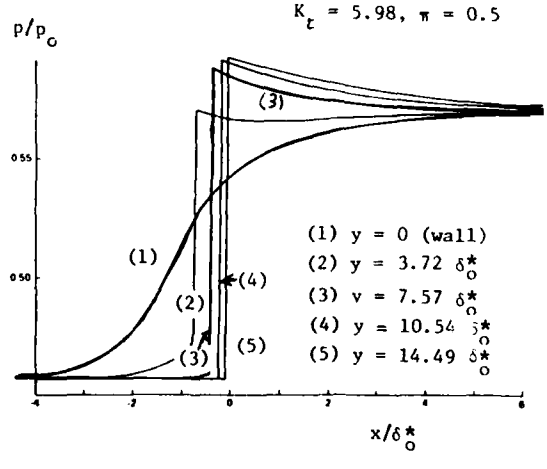

(b) Melnick and Grossman[27]

Fig. 13 Theoretical Pressure Distributions for Normal Shock Interaction in a Straight Pipe

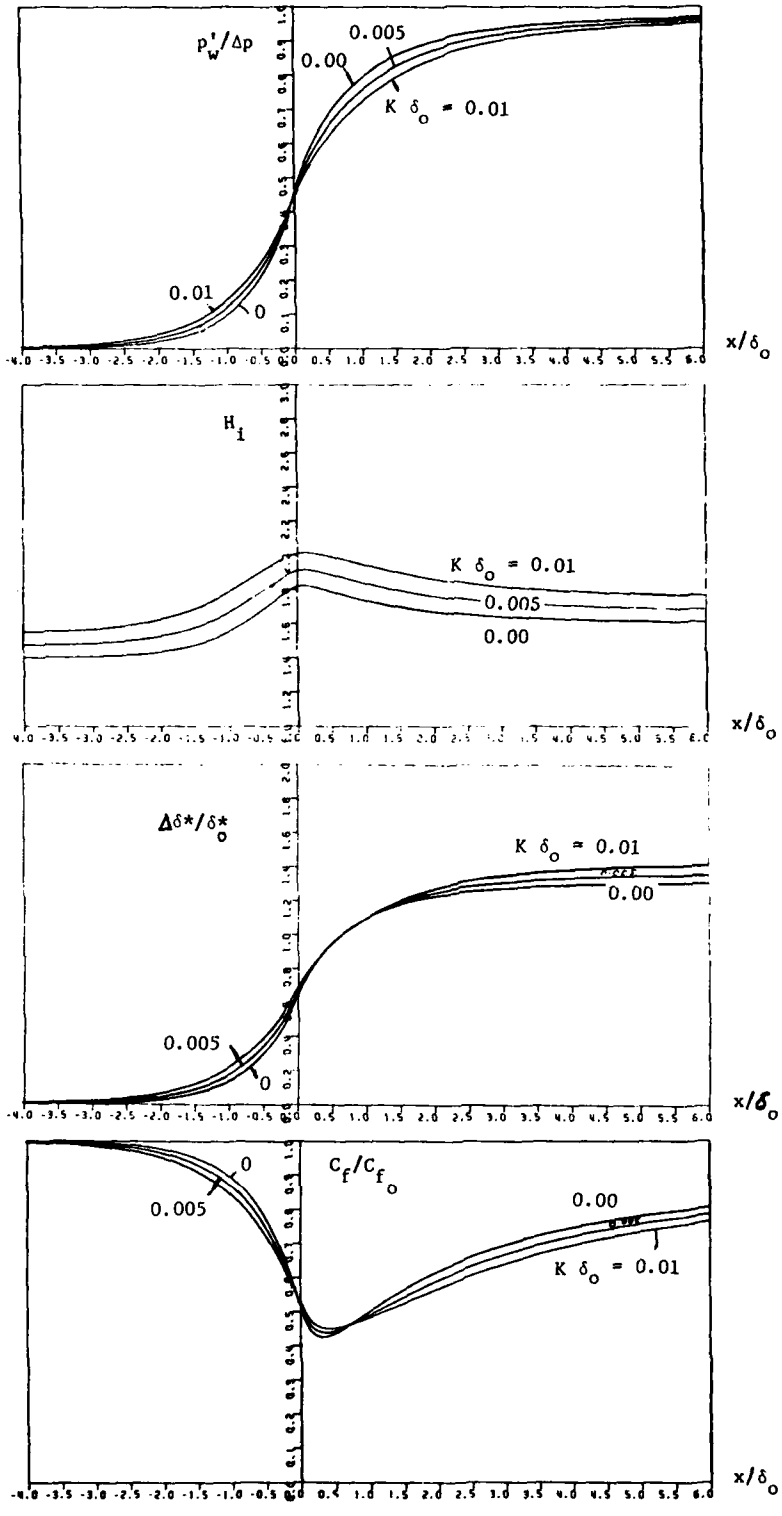

a. Wall Pressure

b. Shape Factor

c. Displacement Thickness

d. Skin Friction

Fig. 14 Typical Results of a Parametric Study of Wall Curvature Effect on Local Interaction Zone Flow Properties ($M_1 = 1.20$, $H_{i_1} = 1.40$, $Re_{\delta^*_o} = 3.5 \times 10^4$)

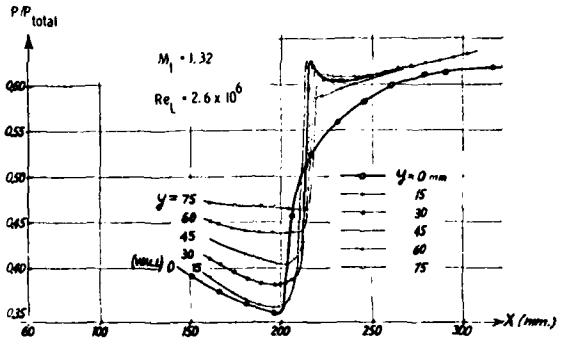

a. Typical Pressure Data

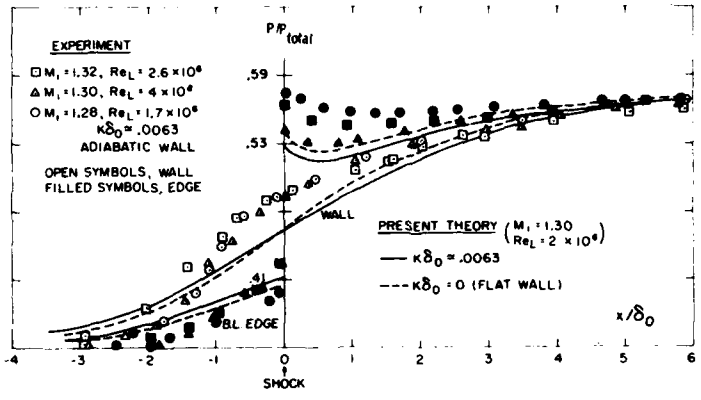

b. Wall and Edge Pressure Comparisons

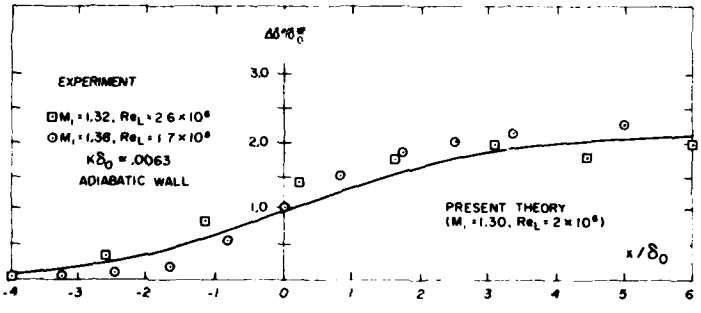

c. Displacement Thickness

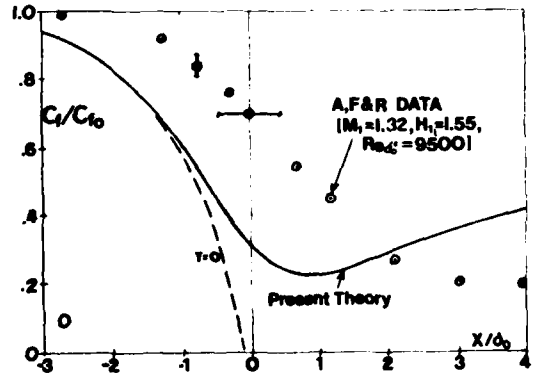

d. Skin Friction

Fig. 15 Comparison of Present Theory With Experimental Interaction Data of Ackert, Feldman and Rott[7]

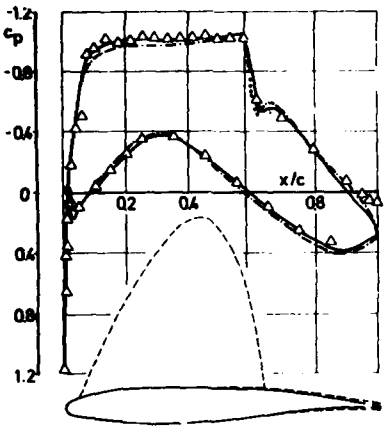

AIRFOIL CAST 7 / DOA 1

$M_\infty = 0.765$
$\alpha_g = 2.4°$
$Re = 2.4 \times 10^6$
Transition at 7% c
WIND TUNNEL: DFVLR-TWB

- Surface pressure due to interaction code

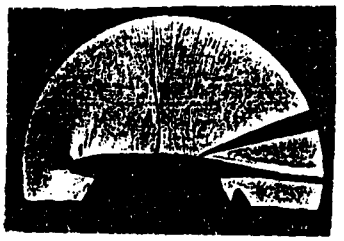

--△--EXPERIMENT
—x— INTERACTION CODE

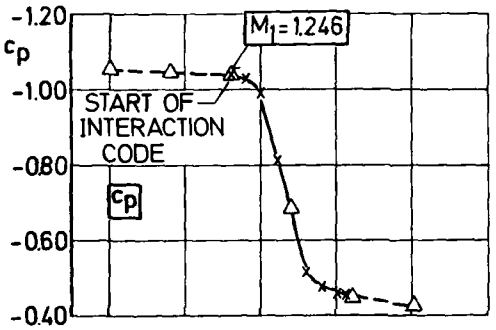

Pressure Distribution

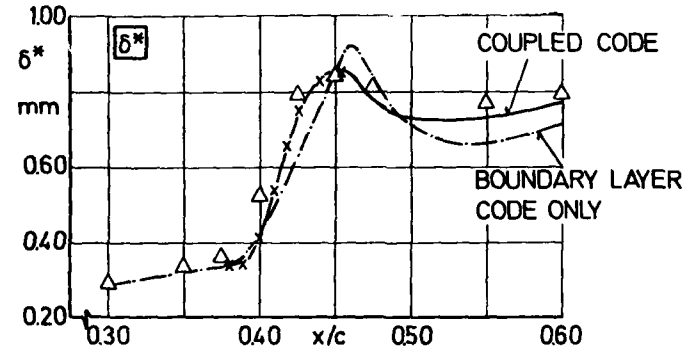

Displacement Thickness

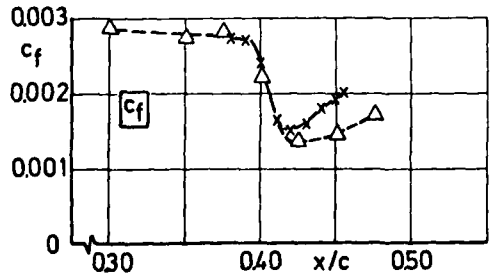

Skin Friction Distribution

Fig. 16 Comparison of Theory and Experiment[22] for the Interaction Zone on a Supercritical Airfoil

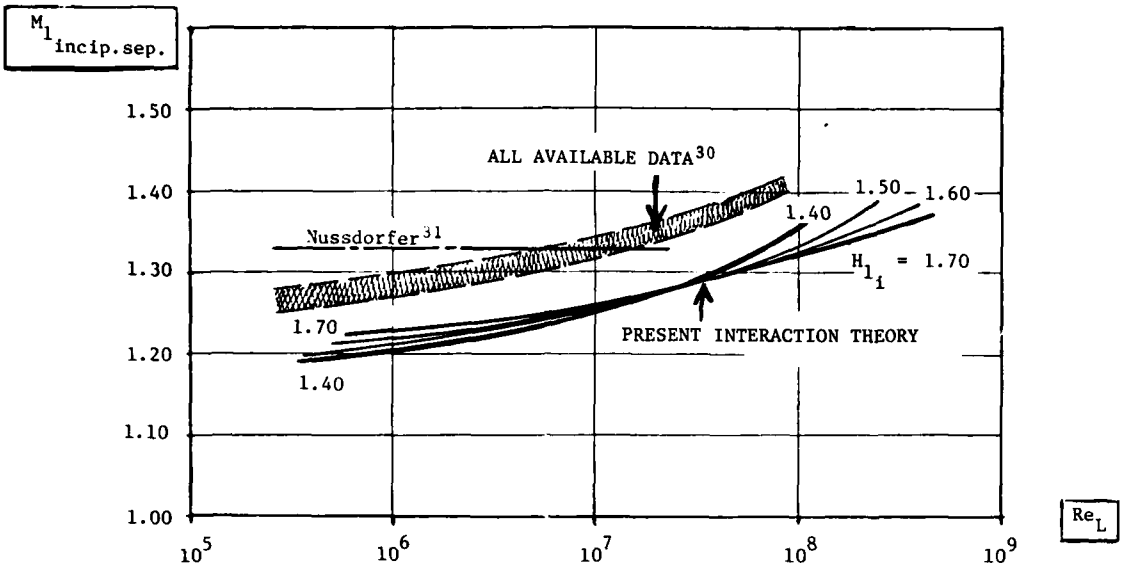

a. Shape Factor Effect ($K\delta_o = 0$)

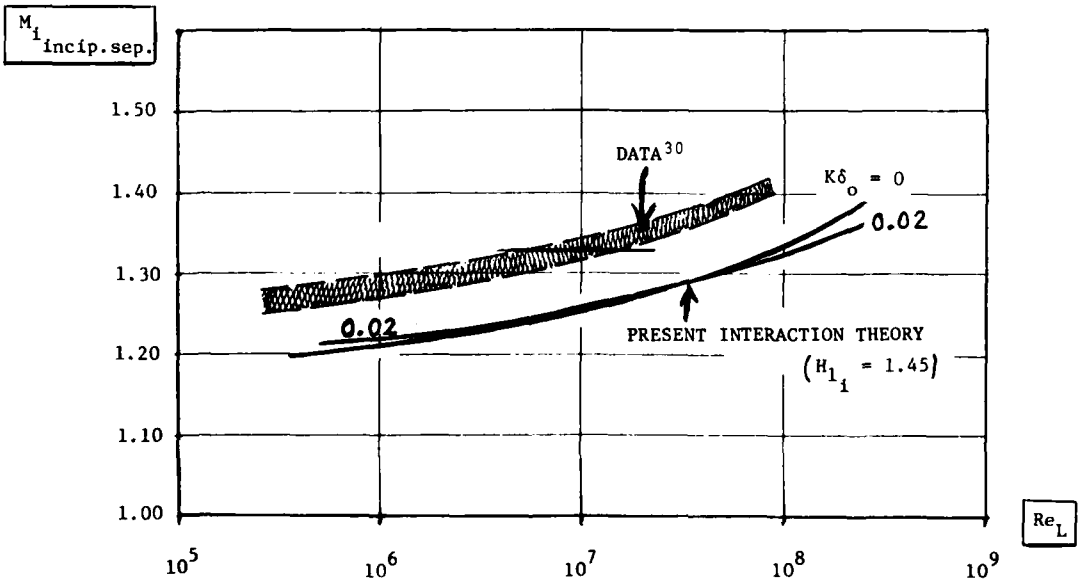

b. Wall Curvature Effect

Fig. 17. Incipient Separation Shock Mach Number vs. Reynolds Number: Comparison of Theoretical Prediction With Experimental Data

Unclassified

SECURITY CLASSIFICATION OF THIS PAGE (When Data Entered)

REPORT DOCUMENTATION PAGE		READ INSTRUCTIONS BEFORE COMPLETING FORM
1. REPORT NUMBER AIAA Paper 81-1244	2. GOVT ACCESSION NO.	3. RECIPIENT'S CATALOG NUMBER
4. TITLE (and Subtitle) TRANSONIC SHOCK - TURBULENT BOUNDARY LAYER INTERACTION AND INCIPIENT SEPARATION ON CURVED SURFACES		5. TYPE OF REPORT & PERIOD COVERED Interim Tech. Rept. 6. PERFORMING ORG. REPORT NUMBER
7. AUTHOR(s) George R. Inger		8. CONTRACT OR GRANT NUMBER(s) ONR N00014-80-C-0470
9. PERFORMING ORGANIZATION NAME AND ADDRESS Dept. of Aerospace Engineering Sciences University of Colorado Boulder, Colorado 80309		10. PROGRAM ELEMENT, PROJECT, TASK AREA & WORK UNIT NUMBERS
11. CONTROLLING OFFICE NAME AND ADDRESS		12. REPORT DATE June 1981 13. NUMBER OF PAGES 20
14. MONITORING AGENCY NAME & ADDRESS (if different from Controlling Office) Office of Naval Research 800 North Quincy Street Arlington, Virginia 22217		15. SECURITY CLASS. (of this report) Unclassified 15a. DECLASSIFICATION/DOWNGRADING SCHEDULE

16. DISTRIBUTION STATEMENT (of this Report)

Distribution unlimited

17. DISTRIBUTION STATEMENT (of the abstract entered in Block 20, if different from Report)

18. SUPPLEMENTARY NOTES

19. KEY WORDS (Continue on reverse side if necessary and identify by block number)

Transonic
Shock-Boundary Layer Interaction
Turbulent
Wall Curvature

20. ABSTRACT (Continue on reverse side if necessary and identify by block number)

A detailed analysis is made of weak normal shock-turbulent boundary layer interactions on longitudinally-curved surfaces for the case of non-separating steady 2-D flow. It is shown that the interactive viscous displacement effect on the local outer inviscid transonic flow eliminates the well-known singularity pertaining to a curved wall. The inner interaction solution within the boundary layer reveals that curvature moderately influences the interaction through the turbulent eddy viscosity. A non-asymptotic triple-deck solution valid over a wide range of practical Reynolds numbers is given which incorporates this

DD FORM 1 JAN 73 1473 EDITION OF 1 NOV 65 IS OBSOLETE
S/N 0102-LF-014-6601

Unclassified

SECURITY CLASSIFICATION OF THIS PAGE (When Data Entered)

40618-1

BLOCK 20, cont.

effect, and example numerical results are presented and verified by comparison with experimental data. Small amounts of curvature ($K \delta_o \lesssim .01 - .02$) are found to moderately spread out and thicken the interaction zone while also delaying slightly the onset of any incipient separation that occurs under the shock.

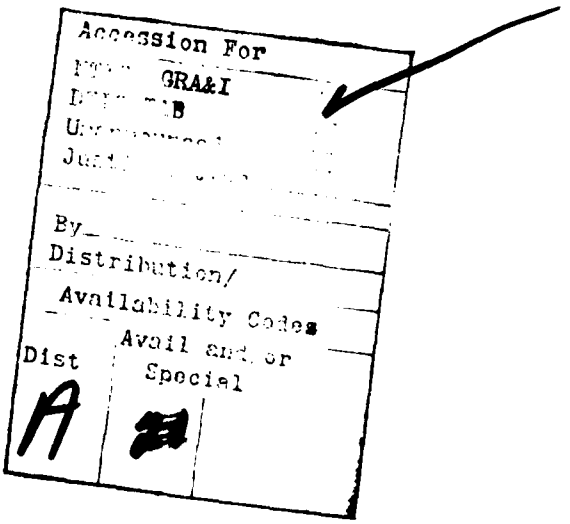


DAT
FILM